Interleukin-1 Receptor Antagonist Protein: Solution Secondary Structure from NOE's and $^{1}H\alpha$ and $^{13}C\alpha$ Chemical Shifts

Brian J. Stockman, Terrence A. Scahill, Annica Euvrard, Nancy A. Strakalaitis, David P. Brunner, Anthony W. Yem, and Martin R. Deibel, Jr.

The Upjohn Company, 301 Henrietta St., Kalamazoo, MI 49007

1 Introduction

Interleukin-1α and interleukin-1β are two polypeptides which share a significant number of inflammatory, immunological and pathological properties (for a review see [1]). Importantly, these dissimilar 17 kDa proteins bind to two classes of interleukin-1 receptors, resulting in the mediation of several immune and inflammatory responses and in the induction of a variety of biological changes in neurologic, metabolic, hematologic, and endocrinologic systems [1]. In addition to IL-1α and IL-1β, an interleukin-1 receptor antagonist protein (termed either IRAP or IL-1ra) has been isolated, characterized, cloned and expressed in *E. coli* [2-4]. This newer member of the IL-1 gene family is a naturally occurring inhibitor of the interleukin-1 receptor [2,4], and represents the first described naturally occurring cytokine that functions entirely as a specific receptor antagonist.

Site-directed mutagenesis [5-7] and protein modification [6] studies have identified three regions of IL-1 that are involved in either receptor binding or transmission of the biological response upon binding. For IRAP, it can be hypothesized that the regions of structure important for receptor binding are maintained, but that the region or regions responsible for eliciting the response are somehow different. To this end, we have begun an intensive program to determine the solution structure of IRAP using NMR spectroscopy. Since the solution [8-12] and crystalline [13,14] structures of IL-1β have been determined, direct comparisons can be made between IRAP and IL-1β. This may lead to a correlation between structural and biological differences.

2 Methods

Expression of IRAP was carried out using *E. coli* K-12 strain DU379. Fermentation media were supplemented with $(^{15}NH_4)_2SO_4$, [$^{13}C_1$]- and/or [^{15}N]-L-methionine, $^{15}NH_4Cl$, and [^{13}C]-D-glucose (stable isotopes were obtained from Cambridge Isotope Laboratories, Isotec, and/or MSD Isotopes) as required to produce either ^{15}N- or doubly $^{13}C/^{15}N$-enriched IRAP. Analysis of resolved ^{1}H resonances indicated that both ^{13}C and ^{15}N were incorporated at an enrichment level greater than 95%. Samples for NMR spectroscopy contained 2 mM IRAP, 50 mM $^{2}H_4$-ethanolamine and 300 mM NaCl at pH 6.4. Trace amounts of PMSF and NaN_3 were added to prevent any protease digestion or bacterial growth in the sample.

All NMR spectra were recorded at 27 °C on a Bruker AMX-600 spectrometer equipped with a triple-resonance probe and a multi-channel interface. Three-dimensional ^{1}H-^{15}N NOESY-HMQC and TOCSY-HMQC experiments were recorded with slight modification of the methods of Zuiderweg and Fesik [15] and Marion et al. [16]. Three-dimensional ^{1}H-^{15}N-^{13}C HNCA and HN(CO)CA triple resonance experiments were recorded with constant-time ^{15}N evolution as described by Grzesiek and Bax [17]. Detailed acquisition parameters have been described elsewhere [18]. Three-

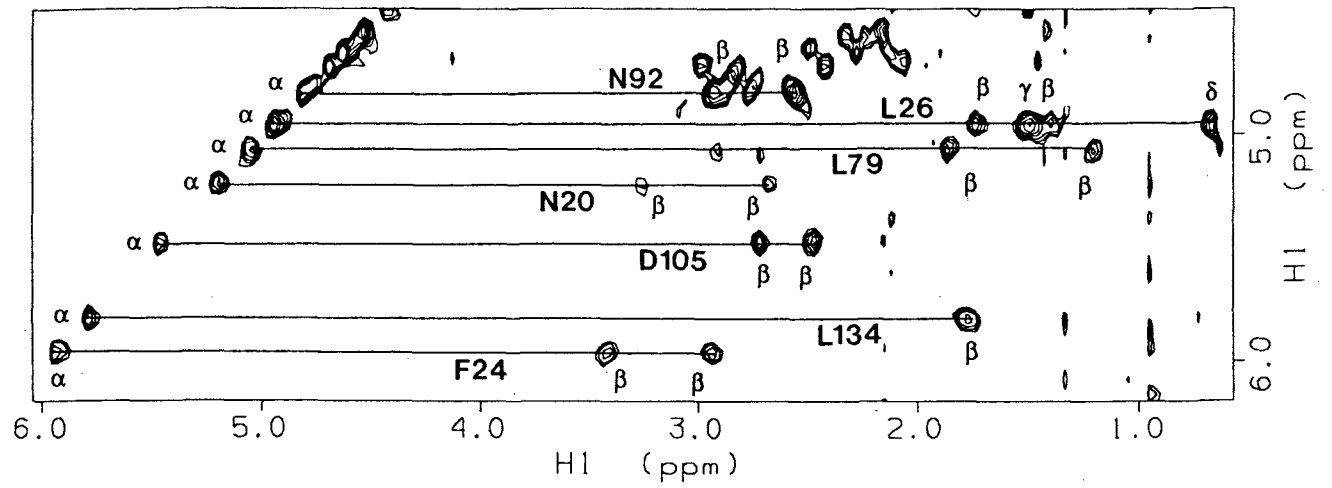

Figure 1. Region of the slice corresponding to ^{13}C frequencies of 18.7 and 51.8 ppm in the ^{1}H-^{13}H-^{13}C-^{1}H TOCSY spectrum of IRAP. Several assigned correlations are labeled.

dimensional ^{1}H-^{13}C-^{13}C-^{1}H COSY [19], ^{1}H-^{13}C-^{13}C-^{1}H TOCSY [20], and ^{1}H-^{13}C NOESY-HMQC [21] experiments were also recorded.

3 Results

Assignment of the majority of the backbone ^{1}H, ^{13}C, and ^{15}N resonances of IRAP was accomplished by analysis of four three-dimensional data sets. First, ^{1}H-^{15}N NOESY-HMQC and TOCSY-HMQC experiments were recorded on uniformly ^{15}N-enriched IRAP. Then, two ^{1}H-^{15}N-^{13}C triple resonance experiments were recorded, the so-called HNCA and HN(CO)CA experiments [22,23]. Redundant sequential connectivities obtained from the heteronuclear data sets simplified and increased the reliability of the assignments. During the assignment process, NOE's indicative of secondary structure were identified.

For many residues, magnetization transfer in the ^{1}H-^{15}N TOCSY-HMQC spectrum extended resonance assignments to at least one $^{1}H\beta$ resonance and sometimes even further down the side chain. In cases of favorable resolution, such as for high-field shifted resonances, two-dimensional DQF-COSY and TOCSY spectra confirmed and/or extended these side-chain assignments. Extensive side-chain assignments, however, will require ^{13}C-directed strategies [19,20] and are currently in progress. A representative slice from the ^{1}H-^{13}C-^{13}C-^{1}H TOCSY spectrum of IRAP is shown in Figure 1.

Once the majority of correlations were assigned in the ^{1}H-^{15}N HSQC spectrum recorded in $^{1}H_2O$, an identical spectrum was recorded after exchanging the protein into $^{2}H_2O$. Only 50 ^{1}H-^{15}N correlations remained after six hours in $^{2}H_2O$ solvent. As discussed below, each of these residues was found to participate in the β-sheet framework of IRAP.

4 Discussion

During analysis of the ^{1}H-^{15}N NOESY-HMQC data set, NOE's indicative of the solution secondary structure [24] of IRAP were identified. The majority of these were classified as cross-strand NOE's between residues involved in β-sheet structure. They are manifested in the NOESY-HMQC spectrum as a third $^{1}H^{\alpha}$ NOE to an amide proton (the others being the interresidue and intraresidue $^{1}H^{\alpha}$'s), or as weak, non-sequential $^{1}H^{N}$-$^{1}H^{N}$ NOE's. Stretches of residues giving rise to these types of NOE's also had other characteristics associated with β-sheet residues: low field $^{1}H^{\alpha}$ and $^{1}H^{N}$ chemical shifts, strong $^{1}H^{N}$-$^{1}H^{\alpha}$ coupling (manifested by intense DQF-COSY and TOCSY correlations), and reduced $^{1}H^{N}$ exchange rates. In addition, 22 intense $^{1}H^{\alpha}$-$^{1}H^{\alpha}$ NOE's, characteristic of antiparallel β-sheet [24], were

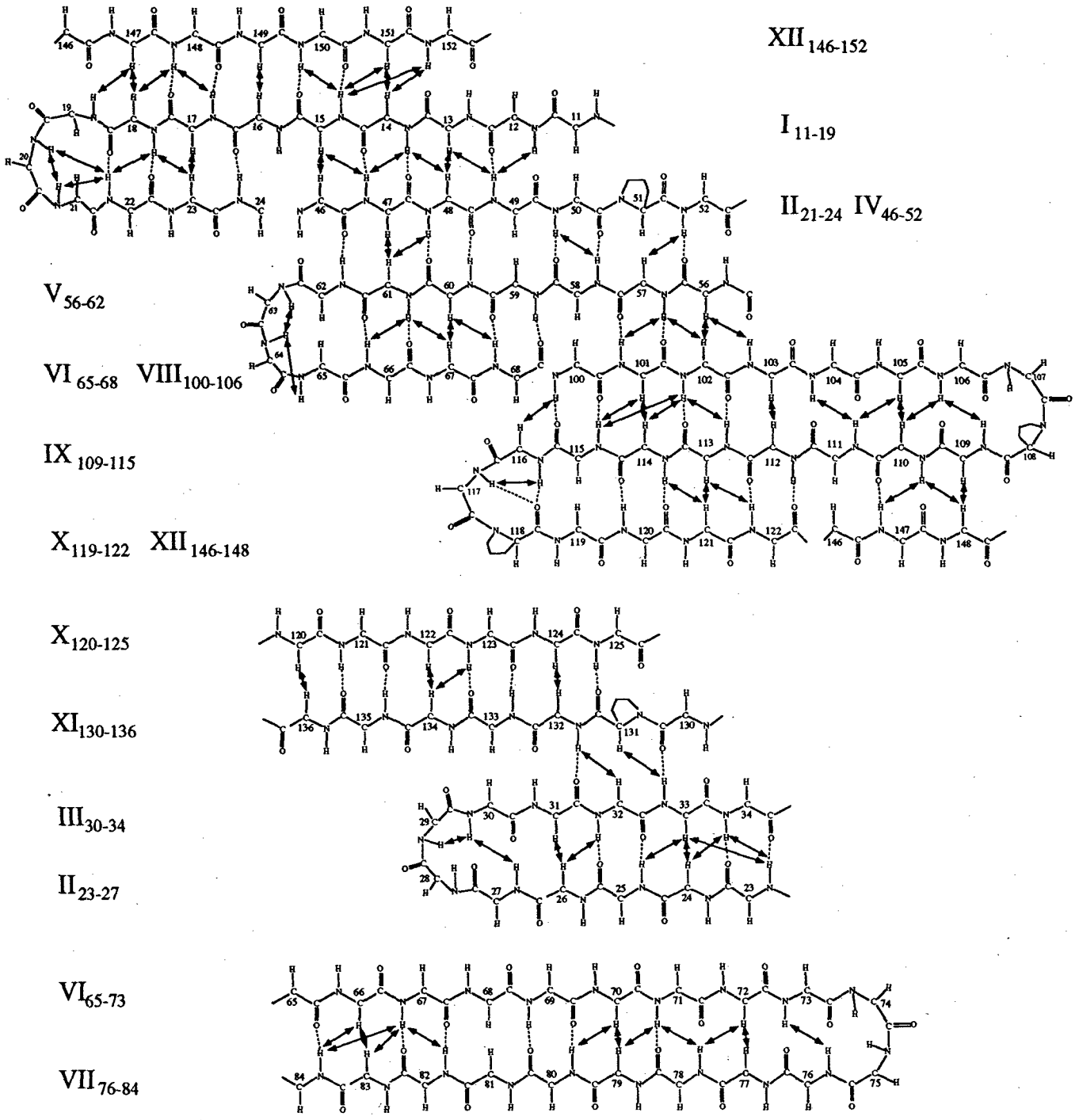

Figure 2. Schematic diagram of the topology of the β-sheet framework of IRAP. Double-arrowhead lines identify assigned inter-strand NOE's. Dashed lines indicate inter-strand hydrogen bonds inferred from analysis of $^{1}H^{N}$ exchange rates.

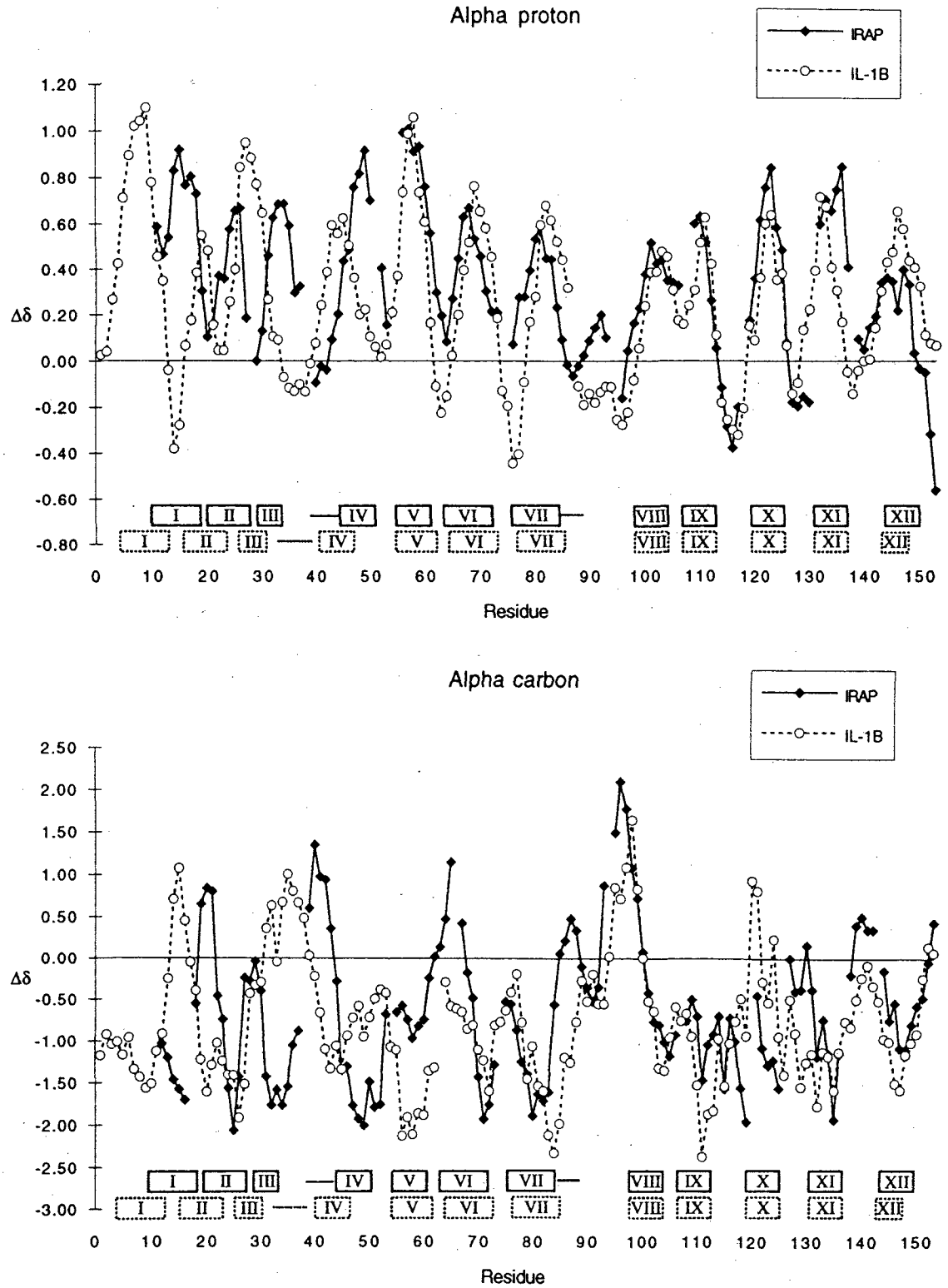

Figure 3. Comparison of $^{1}H^{\alpha}$ (top) and $^{13}C^{\alpha}$ (bottom) $\Delta\delta$ chemical shifts for IRAP and IL-1β. Locations of NOE-defined secondary structure elements in both proteins are shown at the bottom of each plot. β-strands are boxed, while helical regions are denoted by lines.

identified in the two-dimensional NOESY spectrum recorded in ^2H_2O and confirmed in the ^1H-^{13}C NOESY-HMQC spectrum. Analysis of this pattern of NOE's results in alignment of the 12 β-sheet strands as shown in Figure 2. Arrows indicate observed cross-strand NOE's, while dashed lines indicate hydrogen bonds inferred from $^1H^N$ exchange rates.

The β-sheet strands have been presented in Figure 2 in a manner that allows easy comparison to the β-sheet framework elucidated for IL-1β in solution by Driscoll et al. ([9], Figure 5). Comparison of the two figures illustrates how the overall topology of the two proteins is identical, but in several regions is composed of different stretches of the primary sequence. Strands II and III, which are adjacent strands connected by a five-residue turn in IL-1β, are shifted by six residues in the primary sequence and are connected by a four-residue turn in IRAP. Similarly, strands I and IV in IRAP are shifted by six and five residues, respectively. The consequence of shifting the residues that comprise these portions of the β-sheet is that the N-terminal six residues of IRAP have no structural counterpart in the IL-1β structure. Structurally significant shifts of one residue are seen for strands VI, VII, and XII.

As expected for predominantly β-sheet proteins, large positive (downfield) deviations from random coil chemical shifts are observed for the $^1H^\alpha$ resonances [25], and large negative (upfield) deviations from random coil chemical shifts are observed for the $^{13}C^\alpha$ resonances [25,26]. Comparison of the secondary $^1H^\alpha$ and $^{13}C^\alpha$ chemical shifts of IRAP and IL-1β also illustrates the differences and similarities in location of secondary structure elements, as shown in Figure 3. Note the excellent agreement of the out-of-phase appearance of the plots over the first 50 residues with the five- or six-residue offset in location of the β-strands. Also note how the in-phase sections of the plots correspond to β-strands at identical positions in both proteins.

While the solution secondary structure of IRAP is dominated by antiparallel β-sheet, short stretches of strong $^1H^N$-$^1H^N$ NOE's between adjacent residues, indicative of a helical conformation, were also observed. As shown in Figure 2, these regions involve residues 40-45 and 86-89. In addition, NOE's from $^1H^N$ of L89 to $^1H^\alpha$ of I86 and from $^1H^N$ of E44 to $^1H^\alpha$ of V41, both medium-range NOE's characteristic of a helical conformation [24], were observed. These were the only NOE's of this type unambiguously assigned. In addition, the $^{13}C^\alpha$ chemical shifts in these two stretches are shifted downfield slightly compared to their random coil values, as would be expected for a helical conformation [26]. These residues correspond to residues 35-40 and 87-90 in IL-1β, the former of which is a 3_{10} helix in solution [9]. Isolated strong $^1H^N$-$^1H^N$ NOE's between two or three sequential residues were also observed, and locate turn conformations at positions: 18-22, 27-30, 62-65, and 116-118.

5 Acknowledgements

We thank Dr. Paul E. Fagerness, Dr. Eldon L. Ulrich, Dr. Melinda Roy, Kathleen A. Farley, Ron L. VanZanten, and Cindy A. Granatir for their continuing contributions. We thank Dr. Ad Bax (NIH) for advice and for supplying preprints of the constant-time HNCA and HN(CO)CA pulse sequences.

6 References

1. Dinarello, C. A. (1989) *Adv. Immunology 44*, 153-205.
2. Hannum, C. H., et al. (1990) *Nature 343*, 336-340.
3. Eisenberg, S. P., et al. (1990) *Nature 343*, 341-346.
4. Carter, D. B., et al. (1990) *Nature 344*, 633-638.
5. MacDonald, H. R., et al. (1986) *FEBS Lett. 209*, 295-298.
6. Wingfield, P., et al. (1989) *Eur. J. Biochem. 179*, 565-571.
7. Gehrke, L., et al. (1990) *J. Biol. Chem. 265*, 5922-5925.
8. Driscoll, P.C., et al. (1990a) *Biochemistry 29*, 3542-3556.
9. Driscoll, P. C., et al. (1990b) *Biochemistry 29*, 4668-4682.
10. Clore, G. M., Wingfield, P. T., & Gronenborn, A. M. (1991) *Biochemistry 30*,

2315-2323.
11. Clore, G. M, &. Gronenborn, A. M. (1991) *J. Mol. Biol. 221*, 47-53.
12. Tate, S., et al. (1992) *Biochemistry 31*, 2435-2442.
13. Finzel, B. C., et al. (1989) *J. Mol. Biol. 209*, 779-791.
14. Priestle, J. P., Schår, H. P., & Grütter, M. G. (1989) *Proc. Natl. Acad. Sci. U.S.A. 86*, 9667-9671.
15. Zuiderweg, E. R. P., & Fesik, S. W. (1989) *Biochemistry 28*, 2387-2391.
16. Marion, D., et al. (1989) *Biochemistry 28*, 6150-6156.
17. Grzesiek, S., & Bax, A. (1992)*J. Magn. Reson. 96*, 432-440.
18. Stockman, B. J., et al. (1992) *Biochemistry 31*, 5237-5245.
19. Ikura, M., Kay, L. E., & Bax, A. (1991) *J. Biomol. NMR 1*, 299-304.
20. Clore, G. M., et al. (1990) *Biochemistry 29*, 8172-8184.
21. Ikura, M., et al. (1990) *J. Magn. Reson. 86*, 204-209.
22. Ikura, M., Kay, L. E., & Bax, A. (1990) *Biochemistry 29*, 4659-4667.
23. Bax, A., & Ikura, M. (1991) *J. Biomol. NMR 1*, 99-104.
24. Wüthrich, K. (1986) *NMR of Proteins and Nucleic Acids*, Wiley, New York.
25. Wishart, D. S., Sykes, B. D., & Richards, F. M. (1991) *J. Mol. Biol. 222*, 311-333.
26. Spera, S., & Bax, A. (1991) *J. Am. Chem. Soc. 113*, 5490-5492.